# LIFT-FRR Assessment of the Oxidized Size of PQ Pool in PSII Based on the Kinetics of $Q_A^-$ Reoxidation

## *Rationale*

The time-course of $Q_A^-$ reoxidation is frequently expressed in a form of a multi-exponential kinetics:

$$f(t) = \sum_{i=1}^{n} a_i \exp(-r_i t) \tag{1a}$$

$$\sum_{i-1}^{n} a_i = 1\,. \tag{1b}$$

The simple form of this expression makes it amenable for fitting the fluorescence transient data using well-established numerical procedures of least squares or the maximum likelihood method. Linear combination of exponential terms in Eqn. 1a allows efficient calculations of partial derivatives, which represents the most computationally-expensive part of the fitting procedure. At the same time, the assumed multi-exponential model of $Q_A^-$ reoxidation usually produces satisfactory fit of experimental data do the theoretical models describing processes of light absorption, charge separation, and electron transport between PSII and PSI (Kolber et al, 1998).

The form of Eqn. 1a implies presence of n parallel pathways of $Q_A^-$ reoxidation, each operating on $a_i$ fraction of QA, with corresponding rate constant $r_i$. Such interpretation of electron transport between PSII and PSI, however, is incorrect. Instead, a sequential electron transfer along $Q_A$, $Q_B$, and PQ pool pathway represents more reasonable model of events in photosynthesis. Such model is usually described by a set of differential equations, where Eqn. 1a describes a solution for the first state variable representing the reduction status of $Q_A$. The actual properties of the electron transport chain, such as the pool sizes of electron carriers and the rate constants of electron transfer between these carriers, are defined by parameterizing these equations. Here we present one possible approach to this problem.

## *Two-exponential kinetics of $Q_A^-$ reoxidation*

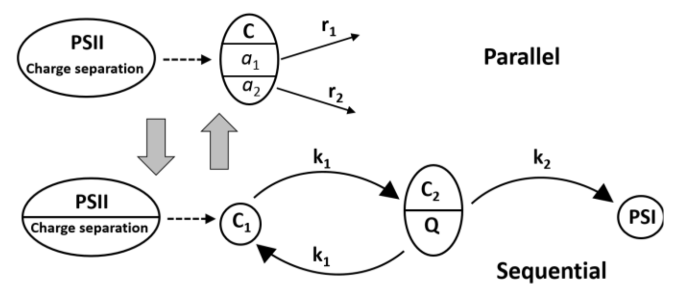

**Fig. 1.** Model of PSII-PSI electron transport based on two-exponential kinetics of $Q_A^-$ reoxidation. The parallel model described by Eqn. 2a assumes two fractions, $a_1$ and $a_2$, of electron acceptor, each reoxidizing with rate constant $r_1$ and $r_2$, respectively. Analytically equivalent model, expressed by Eqns. 3a and 3b, is described by two state variables: $C_1$ representing the redox state of $Q_A$, and $C_2$ representing the redox state of PQ pool. Q is the size of PQ pool in electron equivalents, $k_1$ is rate constant of electron exchange between $Q_A$ and PQ pool, and $k_2$ is rate constant of PQ pool reoxidation.

To simplify our analysis, let's assume that the time-course of $Q_A^-$ reoxidation is expressed in a form of a two-exponential kinetics:

$$f(t) = a_1 \exp(-r_1 t) + a_2 \exp(-r_2 t) \tag{2a}$$

$$a_1 + a_2 = 1\,. \tag{2b}$$

As Eqns. 2a and b contain three independent variables, the corresponding model of sequential electron transport must be described by no more than three parameters. One of several possible models, shown in Fig. 1, is described by the rate constant $k_1$ of redox exchange between $Q_A$ (the $C_1$ state) and PQ pool (the $C_2$ state), by the size of the PQ pool, Q (the capacity of the PQ pool in electron equivalents), and by the rate constant of PQ pool reoxidation, $k_2$. This model can be described by a set of differential equations:

$$\dot{C}_1 = -k_1(C_1 - C_2) \tag{3a}$$

$$\dot{C}_2 = \frac{k_1}{Q}(C_1 - C_2) - k_2 C_2, \tag{3b}$$

where $C_1$ and $C_2$ represent the redox state of $Q_A$ and PQ pool, and $\dot{C}_1$ and $\dot{C}_2$ are their time derivatives, respectively. Here we assume that:

1. The two-stage electron transfer, $Q_A \rightarrow Q_B$ and $Q_B \rightarrow$ PQ pool, are represented by a single $Q_A \rightarrow$ PQ pool step operating with an average rate constant $k_1$.
2. For simplicity, the Q parameters quantifies the size of the *oxidized portion* of the PQ pool in units of electron capacity, not in the units of hydroquinone molecules. The latter can be calculated just by scaling Q down by a factor of two.
3. Changes in the reduction level of PQ pool scale down respective to changes in $Q_A$ reduction level by a factor inversely proportional to the oxidized portion of the PQ pool.
4. The rates of PQ pool reoxidation are not affected by the by the reduction level of electron carriers downstream of PQ pool (this is a rather strong assumption, but the two-exponential kinetics of QA- reoxidation limits the number of state variables to two). Also, $k_2$ represent the collective rate constant of PQ reoxidation, not the rate constant of electron transport along the PQ pool → PSI pathway. The latter, denoted as $k_{2,e}$ is calculated by multiplying $k_2$ by Q, a variable that represents the "effective electron capacity" of the PQ pool .

> ***NOTE:*** *the LIFT-FRR software reports the kinetic of electron transport as time constants, not rate constant. The time constants (inverse of rate constant), in units of $\mu$s, provide more intuitive characterization of the time-scales of events related to photosynthetic electron transport.*

A range of models, with different interpretation of fluorescence data, can be constructed by changing these assumption as long as the number of free parameters doesn't exceed the number of parameters in Eqns. 2a,b. The assumption presented here allow quantifying the rate constants of electron exchange between $Q_A$ and PQ pool, the rate constant of PQ pool reoxidation, and the size of the oxidized portion of the PQ pool. In addition, these assumptions allow calculation of the time course of QA and PQ pool reduction/oxidation.

Let's assume the initial conditions, immediately following reduction of $Q_A$, to be as follows:

$$C_{1(t=0)} = 1 \tag{4a}$$

$$C_{2(t=0)} = 0. \tag{4b}$$

Assumption 4a doesn't necessitate that all reaction centers are reduced following application of the excitation signal. It only implies full reduction of $Q_A$ in these PSII reactions that performs charge separation at $t = 0$. The average level of QA reduction, as reported by the complement of photochemical quenching, $1 - q_P$, is defined by the ratio of PSII reaction centers in $Q_A^-$ state to total number of PSII reaction centers.

With these assumption, Eqn. 2a at $t = 0$ takes a form

$$-a_1 r_1 \exp(-r_1 t) - a_1 r_1 \exp(-r_2 t) = -k_1. \tag{5}$$

As the two exponential terms in Eqn. 5 reduce to 1 at *t = 0*, the rate constant $k_1$ can be expressed as

$$k_1 = a_1 r_1 + a_2 r_2,$$

implying that rate constant of electron exchange between $Q_A^-$ and PQ pool is defined by the *weighted average* of two rate constants in Eqn. 2a.

Next, using Eqn. 3a, we express $C_2$ as

$$C_2 = \frac{\dot{C}_1}{k_1} + C_1, \tag{6}$$

and substitute that into Eqn. 3b

$$\frac{\ddot{C}_1}{k_1} + \dot{C}_1 = -\frac{\dot{C}_1}{Q} - k_2 C_2. \tag{7}$$

Solving this equation for *t= 0* allows expressing Q as

$$Q = \frac{\dot{C}_1 k_1}{\ddot{C}_1 + \dot{C}_1 k_1} = \frac{(a_1 r_1 + a_2 r_2)^2}{a_1 r_1^2 + a_2 r_2^2 - (a_1 r_1 + a_2 r_2)^2}. \tag{8}$$

Calculation of $k_2$ rate constant requires finding an analytical expression for the solution of Eqns. 3a,b. Again, substituting $C_2$ (Eqn. 6) into Eqn. 3b yields

$$\ddot{C}_1 + \dot{C}_1 k_1 = -\frac{\dot{C}_1}{Q} k_1 - k_2\left(\dot{C}_1 + C_1 k_1\right), \tag{9}$$

Which can be rearranged as

$$\ddot{C}_1 + \left(k_1 + k_2 + \frac{k_1}{Q}\right)\dot{C}_1 + k_1 k_2 C_1 = 0. \tag{10}$$

The solution to this equation is given by a linear combination of two exponential terms, calculated as a solution of a second-order “characteristic polynomial”:

$$\exp(-rt)\left[r^2 + \left(k_1 + k_2 + \frac{k_1}{Q}\right) r + k_1 k_2\right] = 0, \tag{11}$$

from which $k_2$ can be calculated. A simpler approach is to recognize that this solution is already calculated by the LIFT-FRR fitting procedure in a form of recovered parameters $a_1$, $a_2$, $r_1$, and $r_2$ (Kolber et al, 1998). Therefore, solving Eqn. 10 for $k_2$

$$k_2 = -\frac{\ddot{C}_1 + \dot{C}_1 k_1\left(1 + \frac{1}{Q}\right)}{C_1 k_1 + \dot{C}_1}, \tag{12}$$

and imposing a condition that this equation must be satisfied by both, $a_1 \exp(-r_1 t)$ and $a_2 \exp(-r_2 t)$, allows calculation of $k_2$. Here, we select the $a_1 \exp(-r_1 t)$ component as the solution for $C_1$, yielding

$$k_2 = \frac{r_1 k_1\left(1 + \frac{1}{Q}\right) - r_1^2}{k_1 - r_1}. \tag{13}$$

Then, as noted earlier, $k_{2,e}$, the rate constant of electron transport between PQ pool and PSI, is calculated as

$$k_{2,e} = k_{2,e} Q \, . \tag{14}$$

## *Results*

As mentioned earlier, the model of sequential electron transport proposed in Fig. 1. represent one of the possible interpretations of multi-exponential kinetics of $Q_A^-$ reoxidation. The validity of this model, and the subsequent interpretation of model data needs to be verified experimentally. The most relevant property of this models is the ability to calculate the size of the oxidized PQ pool. This ability can be tested experimentally by performing LIFT-FRR measurements under condition of selective illumination with weak blue (450-480nm) and IR (730 nm) light, and to observe the effect of such illumination on the calculated size of PQ pool. The rationale for using “weak”, less than 5 µm q $m^{-2}s^{-1}$ light, is to modify the balance between activation level of PSII and PSI, while maintaining the photochemical quenching and the state transition status at a level close to a “dark adapted” state. The LIFT-FRR fluorescence transient recorded at varying combination of the blue and IR light display distinctively different kinetics of $Q_A^-$ reoxidation (Fig. 2), with the associated changes in the calculated size of oxidized portion of PQ pool. There are also differences in the in the amplitude and the shape of the saturation portion of the fluorescence transient. The higher amplitude, and the presence of a rising trend observed in in the two lowest setting of the IR light indicate the possible effect of QB site occupancy (or rather “un-occupancy”) under blue light illumination, consistent with higher level of PQ pool reduction.

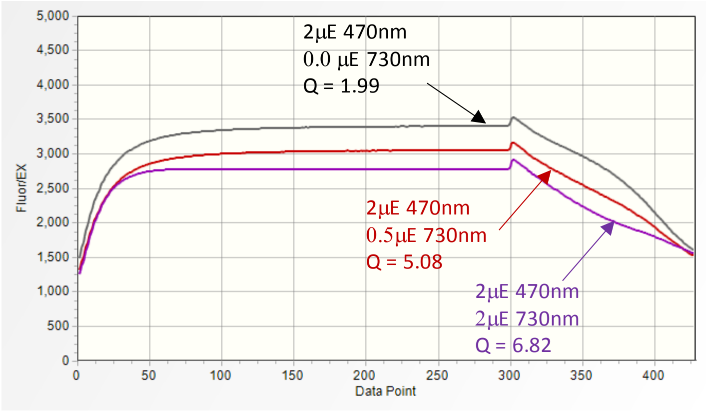

**Fig. 2.** LIFT-FRR fluorescence transients acquired at varying combination of the blue (470 nm) light and the IR (730 nm) light observed on a dark-adapted leaf of a young lemon tree, and the corresponding levels of oxidized portion of the PQ pool. The change in the IR/blue ratio affects the shape of the saturation, as well as the relaxation portion of the observed fluorescence transient. The calculated size of oxidized PQ pool increases with the fraction of IR light, as PSI becomes progressively engaged.

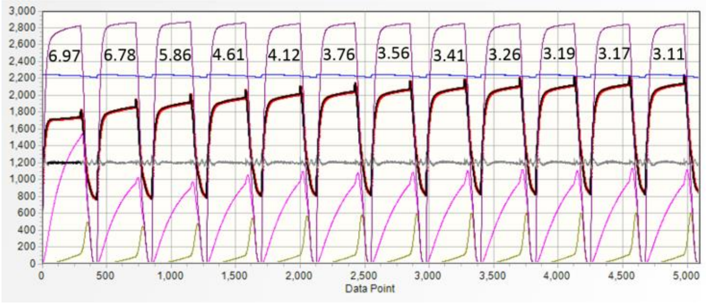

**Fig. 3.** LIFT-FRR fluorescence transients acquired using a sequence of twelve flashes in the dark, on IR (4 µE, at 730nm) pre-illuminated leaf of a lemon tree. Flashes were applied at 1 second interval. The calculated size of the oxidized portion of the PQ pool, obtained by fitting the LIFT-FRR model (dark trace) into the experimental data (red dots) are shown on the top of each flash.

Application of the LIFT-FRR excitation protocol can potentially modify the ambient level of PQ reduction. To quantify this effect, a series of flashes was applied in a 1 second succession on IR pre-illuminated leaf. About 3% decrease in the oxidized portion of the PQ pool was observed between the first and the second flash (Fig 3). Much larger change (equivalent to ~1 electrons) was observed between the subsequent three flashes, presumably due to combination of sufficient time, and the engagement of the two-electrons gate on QB, resulting in progressive filling of the PQ pool with electrons arriving from $Q_A^-$. These changes have saturated at the 10-th flash, when the rates of PQ pool reoxidation balanced the rates of electron delivery to the PQ pool. The amplitude of the fluorescence signal also saturated, consistent with the notion that the level of PQ pool reduction stabilized after the 10-th flash.

The observation presented in Fig. 3 indicate that reliable assessment of the oxidized portion of the PQ pool requires a short excitation protocol that will minimally affect the redox status of the PQ pool (ideally, a single-turnover flash with one charge-separation event). Incidentally, similar requirements need to be satisfied for assessing the functional absorption cross section of PSII. The model described by Eqns. 3a and 3b allows monitoring, in real-time, the state variables $C_1$ ($Q_A$ reduction level) and $C_2$ (PQ pool reduction level). The LIFT-FRR fitting procedure displays these variables, allowing assessing whether, and to what extent, this requirement is satisfied.

## *Kinetics of PQ pool reduction/oxidation*

The ability to quantify the oxidized level of PQ pool *in situ* allows observing the dynamics of PQ pool reduction/oxidation in real-time, non-invasively, with high time resolution. An example of such measurement, performed at 80 cm distance on a dark-adapted, attached leaf of a lemon tree, with flashes applied at 2 seconds interval, indicate fast, less than 2 seconds change in PQ pool reduction level in response to application of IR light (Fig. 4, black trace). The undershoot in the oxidized portion of PQ pool after removal of IR light is associated with transient increase in the time constant of electron

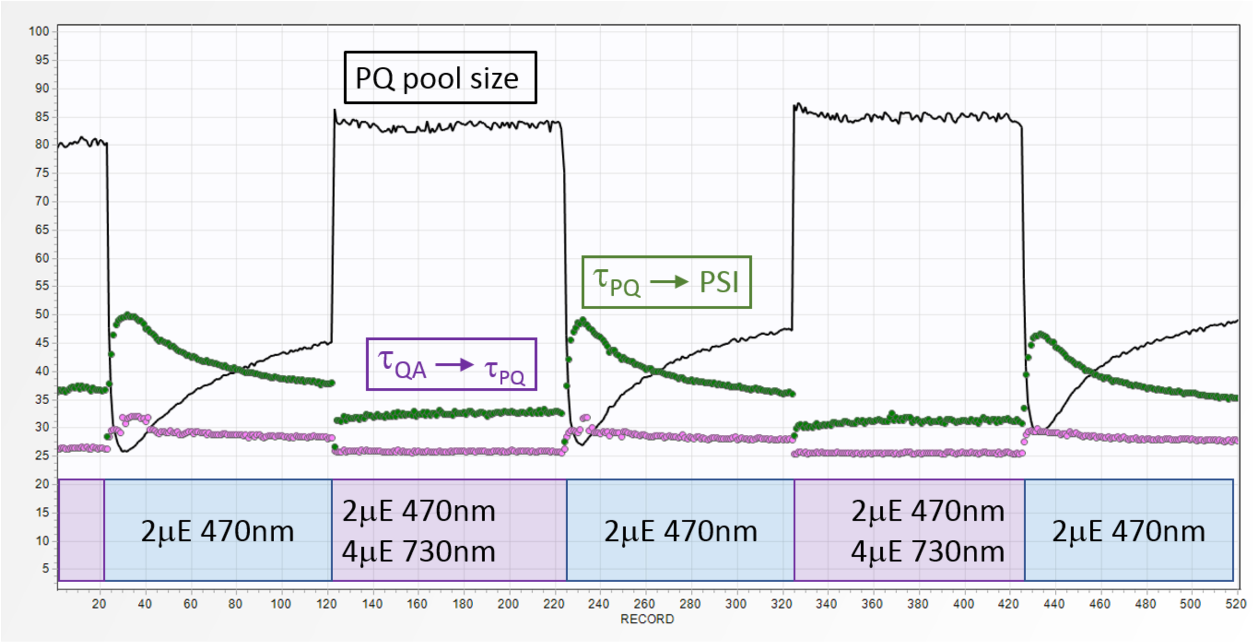

**Fig. 4.** Dynamics of PQ pool oxidation level in response balance shift in activation of PSII and PSI. The size of the oxidized portion of PQ pool varies from ~2.5 to 8.5 (full scale of 10), responding within two seconds after applying, and removing the IR light. The time constants of $Q_A \rightarrow$ PQ pool, and PQ pool→ PSI generally decrease under conditions of oxidized PQ pool (full scale of 4 ms).

transport from PQ pool to PSI (Fig. 4, green dots). The time constant of $Q_A$ → PQ pool electron transport (purple dots in Fig. 4) decreases slightly as PQ pool becomes more oxidized.

## *Three-exponential kinetics of $Q_A^-$ reoxidation*

When the kinetics of $Q_A^-$ reoxidation is expressed in a form of a three-exponential decay, the five parameters retrieved form the fitting procedure allows expressing the electron transport between PSII and PSI using a set of three differential equations:

$$\dot{C}_1 = -k_1(C_1 - C_2) \tag{15a}$$

$$\dot{C}_2 = \frac{k_1}{Q_B}(C_1 - C_2) - k_2(C_2 - C_3), \tag{15b}$$

$$\dot{C}_3 = \frac{k_2}{Q}(C_2 - C_3) - k_3 C_3, \tag{15b}$$

equivalent with the model presented in Fig. 2.

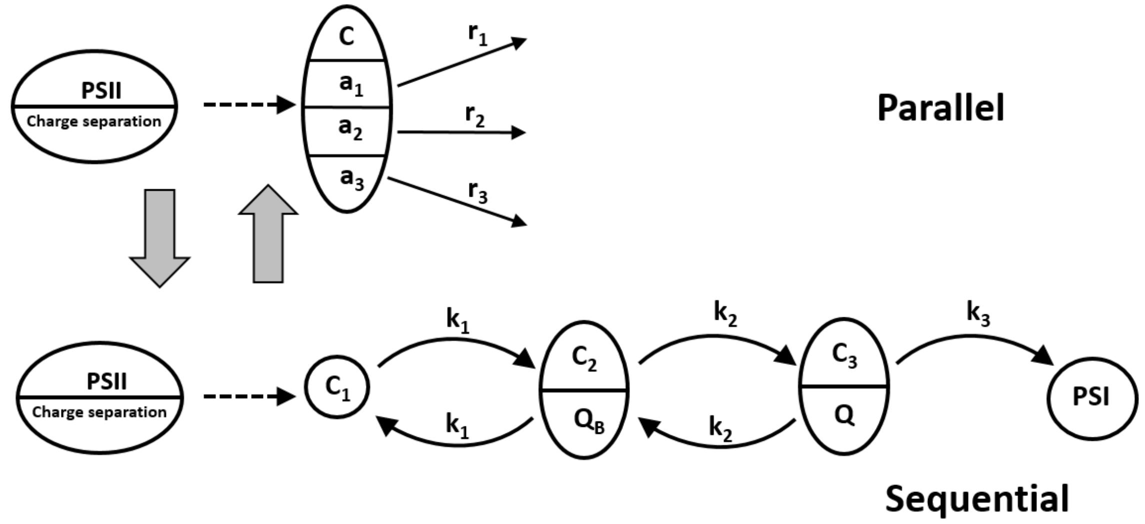

**Fig. 5.** Model of PSII-PSI electron transport based on three-exponential kinetics of $Q_A^-$ reoxidation. The parallel model assumes partition of electron acceptor into three fractions, $a_1$, $a_2$, and $a_3$, each oxidizing with rate constant $r_1$, $r_2$, and $r_3$, respectively. The equivalent sequential model, expressed by Eqns. 15a, b, and c, is described by three state variables: $C_1$ representing the redox state of $Q_A$, $C_2$ representing redox state of QB, and $C_3$ representing the redox state of PQ pool. $Q_B$ is the size of QB pool (assumed to be 2 based on the well-established notion of the two-electron gate), and Q is the size of oxidized PQ pool. The $k_1$ and $k_2$ are rate constants of electron exchange between QA and QB, and between QB and PQ pool, respectively, while $k_3$ is the rate constant of PQ pool reoxidation.

The *$C_1(t)$* can be expressed as linear combination of three exponential components representing a solution of a third-order characteristic polynomial. The mathematical treatment is similar to that described in the previous section, but with few more steps. Fixing $Q_B$ at a value of 2 (assuming a two-electron gate at QB level) allows introducing additional parameter into this model, possibly allowing assessing the occupancy status of the QB pocket on D1 protein. This, however, may lead to under-constraining the model under conditions of low signal-to-noise ratio in the raw fluorescence data.

## *Caveats*

The assumption of multi-exponential kinetics of $Q_A^-$ reoxidation (Eqns. 1a and 1b), although allowing reasonable fitting of experimental data, represents approximate description of $Q_A^-$ reoxidation process. Other models of $Q_A^-$ reoxidation may better satisfy the fitting criteria, while providing different interpretation of the electron transport chain between PSII and PSI. These models are generally described by sets of nonlinear differential equations, requiring purely numerical treatment for integration and calculation of partial derivatives in the fitting procedure. While this increases the numerical effort by about order of magnitude, such purely numerical approach offers high flexibility in model design. This flexibility, however, comes with a danger of under-constraining the numerical procedure by allowing too many free parameters. This problem can be partially controlled by assessing whether the signal-to-noise ratio in the raw fluoresce data permits presence of additional parameters, by observing the fitting criteria as new parameters are introduced, and by analyzing the distribution of residuals along the fluorescence transient data.